



Published in final edited form as:

J Mol Med (Berl). 2013 January ; 91(1): 25–36. doi:10.1007/s00109-012-0968-y.

TRAIL-Death Receptor 4 Signaling via Lysosome Fusion and Membrane Raft Clustering In Coronary Arterial Endothelial Cells: Evidence from ASM Knockout Mice

Xiang Li*, Wei-Qing Han*, Krishna M. Boini, Min Xia, Yang Zhang, and Pin-Lan Li
Department of Pharmacology & Toxicology, Medical College of Virginia Campus, Virginia Commonwealth University

Abstract

Tumor necrosis factor (TNF)-related apoptosis inducing ligand (TRAIL) and its receptor death receptor 4 (DR4) have been implicated in the development of endothelial dysfunction and atherosclerosis. However, the signaling mechanism mediating DR4 activation and leading to endothelial injury remains unclear. We recently demonstrated that ceramide production via hydrolysis of membrane sphingomyelin by acid sphingomyelinase (ASM) results in membrane raft (MRs) clustering and formation of important redox signaling platforms, which play a crucial role in amplifying redox signaling in endothelial cells leading to endothelial dysfunction. The present study aims to investigate whether TRAIL triggers MR clustering via lysosome fusion and ASM activation, thereby conducting transmembrane redox signaling and changing endothelial function. Using confocal microscopy, we found that TRAIL induced MR clustering and its colocalization with DR4 in coronary arterial endothelial cells (CAECs) isolated from wild-type (*Smpd1^{+/+}*) mice. Further, TRAIL triggered ASM translocation, ceramide production and NADPH oxidase aggregation in MR clusters in *Smpd1^{+/+}* CAECs, whereas these observations were not found in *Smpd1^{-/-}* CAECs. Moreover, ASM deficiency reduced TRAIL-induced $O_2^{\cdot-}$ production in CAECs and abolished TRAIL-induced impairment on endothelium-dependent vasodilation in small resistance arteries. By measuring fluorescence resonance energy transfer (FRET), we found that Lamp-1 (lysosome membrane marker protein) and ganglioside G_{M1} (MR marker) were trafficking together in *Smpd1^{+/+}* CAECs, which was absent in *Smpd1^{-/-}* CAECs. Consistently, fluorescence imaging of living cells with specific lysosome probes demonstrated that TRAIL-induced lysosome fusion with membrane was also absent in *Smpd1^{-/-}* CAECs. Taken together, these results suggest that ASM is essential for TRAIL-induced lysosomal trafficking and fusion with membrane and formation of MR redox signaling platforms, which may play an important role in DR4-mediated redox signaling in CAECs and consequent endothelial dysfunction.

Keywords

TRAIL; lysosome fusion; acid sphingomyelinase; membrane raft; endothelial cell; vasorelaxation

Correspondence should be addressed to: Yang Zhang, Ph.D, Department of Pharmacology & Toxicology, Medical College of Virginia Campus, Virginia Commonwealth University, Richmond, VA 23298 Tel: (804) 828-0738, Fax: (804) 628-3765, yzhang3@vcu.edu.
Pin-Lan Li, M.D, Ph.D, Department of Pharmacology & Toxicology, Medical College of Virginia Campus, Virginia Commonwealth University, Richmond, VA 23298 Tel: (804) 828-4793, Fax: (804) 828-4794, pli@vcu.edu.

*These authors contribute equally to this work

Disclosure of potential conflict of interests The authors declare no conflict of interests related to this study.

Introduction

The tumor necrosis factor (TNF)-related apoptosis inducing ligand (TRAIL) is expressed as a type II TNF ligand transmembrane protein, which can be released as a vesicle-associated form or a soluble form. Five receptors for TRAIL have been identified. Two death receptors, DR4 and DR5, contain a death domain and transmit an apoptotic signal in response to TRAIL [1]. Two decoy receptors (DcR1 and DcR2) bind TRAIL without activation of the apoptotic machinery and seem to antagonize DR4 and DR5 [2]. Lastly, osteoprotegerin, originally identified as a regulator of osteoclastogenesis, was shown to bind TRAIL and function as a soluble TRAIL receptor [3]. Endothelial cells (ECs) express all TRAIL receptors including DR4 and DR5, and activation of these receptors has been implicated in the regulation of EC activities including inflammation, proliferation, differentiation and apoptosis [4–8]. For example, TRAIL down-modulated CCL8 and CXCL10 chemokine expression in human umbilical vein endothelial cells (HUVECs), which may contribute to its anti-inflammatory activity by counteracting the ability of TNF- α to promote leukocyte adhesion to ECs [5]. TRAIL induced apoptosis in HUVECs, human dermal and cerebral microvascular ECs [6–8]. In contrast, in HUVECs and human aortic ECs, TRAIL has been shown to activate Akt and ERK1/2 pathways which may be associated with EC proliferation and differentiation [4]. Thus, these findings indicate that TRAIL may in parallel modulate apoptotic pathways as well as antiapoptotic/proinflammatory pathways in ECs. Although these studies revealed the biological activities of TRAIL on ECs, it remains unknown whether and how this death factor indeed produces endothelial dysfunction when it acts on intact vessels for a short time.

Membrane rafts (MRs, previously as lipid rafts) are dynamic assemblies of cholesterol, lipids with saturated acyl chains, such as sphingolipids and glycosphingolipids, in the exoplasmic leaflet of the membrane bilayer, and cholesterol in the inner leaflet [9]. Recently, accumulating evidence suggest that MR clustering is a novel mechanism mediating and amplifying the transmembrane signaling in response to various stimuli in a variety of cell types, including lymphocytes, endothelial cells, and neurons [10–12]. Clustered MRs form membrane signaling platforms, in particular, the ceramide-enriched platforms or macrodomains [9]. These membrane platforms can recruit or aggregate various signaling molecules such as small G proteins, tyrosine kinases, and phosphatases, resulting in the activation of different signaling pathways [9]. More recently, there are increasing evidence that MR clustering on the coronary arterial endothelial cells (CAECs) is an important initiating mechanism in endothelial injury in response to damaging factors such as death receptor agonists, inflammatory factors, irradiation [9, 11, 13]. It has been shown that MR clustering recruits or aggregates redox signaling molecules such as NADPH oxidase subunits, gp91^{phox}, p47^{phox}, and Rac GTPase, resulting in the formation of a membrane signal amplification platform that activates and enhance production of O₂⁻ [11, 14]. These MR signaling platforms associated with O₂⁻ production have been referred as MR redox signaling platforms. The formation of such MR redox signaling platforms in the EC membrane is associated with ceramide production via lysosomal acid sphingomyelinase (ASM), which is translocated onto the plasma membrane via membrane proximal lysosome trafficking and fusion upon stimulation of death receptors [15–17]. Ceramides spontaneously fuse MRs into large ceramide-enriched membrane domains or platforms, which can serve as MR redox signaling platforms [9, 14]. TRAIL has been demonstrated to stimulate ceramide production through ASM and consequent formation of ceramide-enriched platforms in non-endothelial cells [18]. Based on these observations, the present study hypothesized that TRAIL stimulates O₂⁻ production through the formation of the MR redox signaling platforms in CAECs leading to impairment of endothelium-dependent vasodilation and endothelial injury. We used a series of molecular and physiological approaches to test this hypothesis. Particularly, the roles of ASM in lysosome fusion with

plasma membrane, the formation of MR redox signaling as well as TRAIL-induced endothelial impairment were examined in primary cultured CAECs and small resistance arteries isolated from ASM-deficient mice, respectively.

Materials and Methods

Isolation of Mouse Coronary Arterial Endothelial Cells

Isolation and characterization of mouse coronary endothelial cells were performed as described previously [19]. Briefly, the heart was excised with an intact aortic arch and immersed in a petri-dish filled with ice-cold Krebs-Henseleit (KH) solution (mM): 118 NaCl, 1.2 MgSO₄, 1.2 KH₂PO₄, 25 NaHCO₃, 2.5 CaCl₂, and 11 glucose. Surrounding fat and connective tissue were removed from the heart. The cleaned heart with intact aorta was transferred to another petri-dish with fresh KH solution. A 25-gauge needle filled with HBSS (in mM: 5.0 KCl, 0.3 KH₂PO₄, 138 NaCl, 4.0 NaHCO₃, 0.3 Na₂HPO₄·7H₂O, 5.6 D-glucose, and 10.0 HEPES, with 2% antibiotics) was inserted into the aortic lumen opening while the whole heart remained in the ice-cold buffer solution. The opening of the needle was inserted deep into the heart close to the aortic valve. The aorta was tied with the needle as close to the base of the heart as possible. The infusion pump was started with a 20-ml syringe containing warm HBSS at a rate of 0.1 ml/min and the heart was then flushed for 15 min. HBSS was replaced with warm enzyme solution (1 mg/ml collagenase type I, 0.5 mg/ml soybean trypsin inhibitor, 3% BSA, and 2% antibiotic-antimycotic), which was flushed through the heart at a rate of 0.1 ml/min. Perfusion fluid was collected at 30-, 60-, and 90-min intervals. At 90 min, the heart was cut with scissors, and the apex was opened to flush out the cells that collected inside the ventricle. The fluid was centrifuged at 1,000 rpm for 10 min, the cell-rich pellets were mixed with the one of the media described below, and the cells were planted in 2% gelatin-coated six-well plates and incubated in 5% CO₂-95% O₂ at 37°C. Medium 199-F-12 medium (1:1) with 10% FBS and 2% antibiotics was used for isolated endothelial cells. The medium was replaced 3 days after cell isolation and then once or twice each week until the cells grew to confluence. All biochemical studies in the present study were performed using CAECs of two to four passages. CAECs were identified by Dil-Ac-LDL staining as described previously [19, 20]. Six-week-old male C57BL/6J ASM-deficient (*Smpd1*^{-/-}; *Smpd1* is the gene symbol for ASM gene *sphingomyelin phosphodiesterase 1*) mice and their wild-type littermates (*Smpd1*^{+/+}) were used in the present study and mouse genotyping were performed as we described previously [21]. All animals were provided standard rodent chow and water ad libitum in a temperature-controlled room. All protocols were approved by the Institutional Animal Care and Use Committee of Virginia Commonwealth University (Richmond, VA).

Immunofluorescent Microscopic Analysis of MR Clusters

CAECs were grown on poly-L-lysine-coated glass coverslips. After fixation with 4% PFA, cells were incubated with Alexa Fluor 488 conjugated Cholera toxin B (Alexa488-CTXB, 2 µg/mL, 2 h, Molecular Probes, CA), which binds with the MR-enriched ganglioside G_{M1}. For dual-staining detection of the colocalization of MRs with DR4/5, ASM, ceramide or gp91^{phox}, the cells were first incubated with Alexa488-CTXB and then with anti-DR4 or DR5 (1: 250, BD Biosciences, CA), anti-ASM (1: 200, Santa Cruz, CA), anti-ceramide (1: 200, Enzo Life Sciences, NY), and anti-gp91^{phox} (1: 200, BD Biosciences, CA), respectively, which was followed by corresponding Alexa555-conjugated secondary antibodies (1: 500, Invitrogen, NY). Then the colocalization were visualized with confocal microscopy. To accurately observe the staining on the cell membrane, these cells were not permeabilized by excluding detergent in the washing and incubation buffer (phosphate buffered saline, PBS). Clustering was defined as one or several intense spots or patches of fluorescence on the cell surface, while unstimulated cells displayed a homogenous

distribution of the fluorescence throughout the membrane. The results were given as percentage of cells showing a cluster as we described previously [11, 22]

Electron Spin Resonance Detection of Endothelial $O_2^{\cdot-}$

Electron spin resonance was performed as we described previously [11]. Gently collected CAECs were suspended in modified Krebs-HEPES buffer (mM): NaCl 99.01, KCl 4.69, $CaCl_2$ 1.87, $MgSO_4$ 1.20, K_2HPO_4 1.03, $NaHCO_3$ 25.0, Na-HEPES 20.0, and glucose 11.1; pH 7.4), supplemented with deferoxamine (100 μ mol/L; metal chelator). Approximately 1×10^6 cells were then incubated with TRAIL (100 ng/L) for 15 min; these cells were subsequently mixed with 1 mL of the $O_2^{\cdot-}$ -specific spin trap 1-hydroxy-3-methoxycarbonyl-2,2,5,5-tetramethylpyrrolidine (CMH) in the presence or absence of manganese dependent superoxide dismutase (SOD, 500 U/mL, Sigma, St. Louis, MO). The cell mixture was then loaded in glass capillaries and immediately kinetically analyzed for $O_2^{\cdot-}$ production for 10 min. The SOD-inhibited fraction of the signal was compared. The ESR settings were as follows: biofield, 3,350; field sweep, 60 G; microwave frequency, 9.78 GHz; microwave power, 20 mW; modulation amplitude, 3 G; 4,096 points of resolution; receiver gain, 100; and kinetic time, 10 min.

Vascular reactivity in *in vitro* perfused and pressurized small resistance arteries

Small mouse mesenteric arteries (3rd-order branch from superior mesenteric artery, ~100 μ m) were dissected from 6-week old mice in ice-cold physiological saline solution (PSS) containing the following composition (in mM): NaCl, 119; KCl, 4.7; $CaCl_2$, 1.6; $MgSO_4$, 1.17; NaH_2PO_4 , 1.18; $NaHCO_3$, 24; EDTA, 0.026; and glucose, 5.5, pH 7.4 and carefully cleaned off of fat and connective tissues under a dissection microscope. Dissected arteries were immediately transferred to a water-jacketed perfusion chamber and cannulated with two glass micropipettes at their *in situ* length as described previously [23]. The outflow cannula was clamped and the arteries were pressurized to 60 mm Hg and equilibrated in PSS at 37°C. PSS in the bath was continuously bubbled with a gas mixture of 95% O_2 and 5% CO_2 throughout the experiment. After a 1 h equilibration period, the arteries were precontracted with phenylephrine (PE, 1–10 nM) until a ~50% of decrease in resting diameter was reached. Once steady-state contraction was obtained, cumulative dose-response curves to the endothelium-dependent vasodilator acetylcholine (10^{-9} to 10^{-5} M) were determined by measuring changes in internal diameter. To induce endothelial impairment, small arteries were perfused with TRAIL (100 ng/mL) in the lumen and incubated for 1 hour. All other drugs were added into the bath solution unless otherwise indicated. The vasodilator response was expressed as the percent relaxation of PE-induced pre-contraction based on changes in arterial internal diameter. The arteries were excluded from statistical analysis if the contractile response to PE was <40% or dilator response to acetylcholine <80%. Internal arterial diameter was measured with a video system composed of a stereomicroscope (Leica MZ8), a charge-coupled device camera (KP-MI AU, Hitachi), a video monitor (VM-1220U, Hitachi), a video measuring apparatus (VIA-170, Boeckeler Instrument), and a video printer (UP890 MD, Sony). The arterial images were recorded continuously with a videocassette recorder (M-674, Toshiba).

Fluorescence Resonance Energy Transfer analysis

FITC/TRITC pairs were used for fluorescence resonance energy transfer (FRET) assay. CAECs were stained with FITC-conjugated anti-Lamp-1 (a lysosomal marker protein) (1:200, BD Biosciences, CA) and TRITC-labeled CTXB (TRITC-CTXB, 2 μ g/mL, 2 h, Molecular Probes, CA) as described above. An acceptor bleaching protocol was used to measure FRET between FITC/TRITC as we described previously [22]. Briefly, after the pre-bleaching image was normally taken, the laser intensity at the excitement wavelength of the acceptor (TRITC) was increased from 50 to 98% and continued to excite the cell sample for

2 min to bleach the acceptor fluorescence. After the intensity of the excitement laser for acceptor was adjusted back to 50%, the post-bleaching image was taken for FITC. A FRET image was obtained by subtraction of the pre-bleaching images from the post-bleaching images and given a dark blue color. After measuring FITC fluorescence intensity of the pre-, post-, and FRET images, the FRET efficiency was calculated through the following equation: $E = (\text{FITC}_{\text{post}} - \text{FITC}_{\text{pre}}) / \text{FITC}_{\text{post}} \times 100\%$.

FM1–43 Fluorescence Quenching

FM1–43 quenching was performed to detect lysosomal fusion to plasma membrane as described previously [22]. CAECs were firstly loaded with 8 μM FM1–43 (Molecular Probes, CA) for 2 h at 37°C. After washing with FBS free medium, a FM1–43 quenching reagent, bromide phenol blue (BPB, 1 mM, Molecular Probes, CA) was added in the extracellular medium. Cells were then stimulated with or without TRAIL and FM1–43 fluorescence was scanned under confocal microscopy (Olympus) with a low power laser (λ excitation=488 nm) to avoid fluorescent bleaching.

Statistics

Data are presented as mean \pm SE. Significant differences between and within multiple groups were examined using ANOVA for repeated measures, followed by Duncan's multiple-range test. A student *t*-test was used to detect significant differences between 2 groups. $P < 0.05$ was considered statistically significant.

Results

TRAIL induces MRs clustering in mouse CAECs

As shown in Figure 1A, representative MR patches in CAECs under resting control condition and during TRAIL (100 ng/ml, 15 min) stimulation were detected by confocal microscopy. Under resting condition, there was only a diffuse fluorescent staining on the cell membrane by Alexa488-CTXB (CTXB specifically binds MR marker ganglioside GM_1), indicating possible distribution of single MRs without clusters for fluorescent spots or patches. However, when these cells were incubated with TRAIL, large fluorescent dots or patches were detected on the cell membrane. These fluorescent patches indicate the formation of MR clusters or macrodomains. The percentage of cells with intense MR clusters was summarized in Figure 1B showing that TRAIL dose-dependently increased MR clustering in CAECs. Since the optimum response of MR clustering was observed with 100 ng/ml TRAIL for 15 min, the same treatment was used in all experiments of the present study if not otherwise mentioned. Figure 1C shows that DR4 colocalized with MR clusters in CAECs upon TRAIL stimulation as detected by a number of large yellow patches or spots in overlaid image. In contrast, no significant colocalization was observed between DR5 and MR clusters in CAECs with TRAIL treatment. The percentage of cells with intense yellow patches was summarized in Figure 1D indicating that DR4 but not DR5 is involved in TRAIL-induced MR clustering in CAECs.

TRAIL triggers ASM translocation and ceramide production in MR clusters

To investigate the spatial relation between MR clusters and ASM or ceramide, CAECs were stimulated with TRAIL and stained with Alexa488-CTX and Alexa555-conjugated antibodies against ASM or ceramide. As shown in Figure 2A–D, confocal microscopy revealed that ASM or ceramide colocalized in MR clusters in *Smpd1*^{+/+} CAECs after TRAIL stimulation. However, such TRAIL-induced colocalization of ASM or ceramide with MR clusters was abolished in *Smpd1*^{-/-} CAECs.

TRAIL-induced NADPH oxidase aggregation in MR clusters requires ASM activity

We next investigate whether TRAIL induces the formation of MR redox signaling platforms by examining the aggregation of gp91^{phox} in MR clusters since gp91^{phox} is a major NADPH oxidase subunit in the plasma membrane of CAECs. As shown in Figure 3A and 3B, TRAIL increased the colocalization between MRs and gp91^{phox} in *Smpd1*^{+/+} CAECs, whereas TRAIL failed to increase such colocalization in *Smpd1*^{-/-} CAECs.

ASM deficiency reduces TRAIL-induced O₂⁻ production in CAECs

To further examine whether TRAIL-induced MR redox signaling is mediated via ASM/ceramide, *Smpd1*^{+/+} or *Smpd1*^{-/-} CAECs were stimulated with TRAIL and O₂⁻ production in these cells was measured by ESR spectrometric analysis. As shown in Figure 4, in *Smpd1*^{+/+} CAECs, TRAIL significantly increased O₂⁻ production by 2.4 folds compared to control. However, there was no significant increase in O₂⁻ production observed in *Smpd1*^{-/-} CAECs with TRAIL treatment.

ASM deficiency reverses TRAIL-induced impairment on endothelium-dependent vasodilation in small resistance arteries

The results above demonstrate that TRAIL activates NADPH oxidase-derive O₂⁻ production via MR redox signaling pathway. To further investigate the functional significance of TRAIL-induced MR redox signaling, we examined the effects of TRAIL on acetylcholine-induced vasodilation response in small mesentery resistance arteries. As shown in Figure 5A, acetylcholine produced a concentration-dependent vasorelaxation in *Smpd1*^{+/+} arteries with a maximal response of 86 ± 2.5% at concentration of 10⁻⁵ M. Incubation of these arteries with TRAIL significantly attenuated acetylcholine-induced vasodilation with the maximal attenuation of arterial diameters by 40%. In contrast, TRAIL failed to attenuate the endothelium-dependent vasodilation to acetylcholine in similar arteries isolated from *Smpd1*^{-/-} mice (Figure 5B).

TRAIL-induced lysosome trafficking to MRs in CAECs is ASM-dependent

We previously reported that lysosome-targeted ASM is able to traffic to and expose to cell-membrane surface, which may lead to MR clustering and NADPH oxidase activation in CAECs in response to various death receptor stimuli such as Fas ligand (FasL) and endostatin [11, 22]. Thus, we tested the hypothesis that TRAIL triggers lysosomal trafficking and fusion with plasma membrane that is involved in ASM translocation, ceramide production and MR redox signaling. As shown in Figure 6A–C, TRAIL significantly increased the FRET (blue images) between FITC-Lamp-1 (lysosome marker) and TRITC-CTXB in *Smpd1*^{+/+} CAECs but not in *Smpd1*^{-/-} CAECs. As summarized in Figure 6D, FRET efficiency between FITC-Lamp-1 and TRITC-CTXB was significantly increased in response to TRAIL stimulation in *Smpd1*^{+/+} CAECs, however, such increase in FRET efficiency was not observed in *Smpd1*^{-/-} CAECs.

ASM deficiency disrupts TRAIL-induced lysosome fusion with plasma membrane

We further investigated whether TRAIL-induced lysosomal trafficking to MRs is followed by lysosomal fusion with plasma membrane and whether ASM is needed for this fusion process. CAECs were loaded with FM1–43, a fluorescence probe accumulated in lysosomes, and then incubated in fresh culture medium containing BPB, which binds FM1–43 and quenches its fluorescence. As shown in Figure 7A and 7C, TRAIL induced significant decrease in FM1–43 fluorescence *Smpd1*^{+/+} CAECs indicating that lysosome fuses with plasma membrane and exposes of its contents to extracellular spaces. However, TRAIL did not decrease FM1–43 in *Smpd1*^{-/-} CAECs (Figure 7B and 7C). These results indicated that TRAIL-induced lysosome fusion requires ASM activity.

Discussion

The present study demonstrates that death receptor ligand, TRAIL, triggers MRs clustering, formation of MR redox signaling platforms, and activation of NADPH oxidase and production of $O_2^{\cdot-}$ in these platforms in isolated mouse CAECs and induces impairment in endothelium-dependent vasodilation in isolated and pressurized small resistance arteries. In addition, ASM deficiency abolishes these TRAIL-induced signaling events in CAECs and impairment in arteries. These data suggest a novel role of lysosomal ASM-mediated MR redox signaling in the action of TRAIL on ECs and TRAIL-induced endothelial injury.

MR clustering was first visualized on the cell membrane of CAECs by confocal microscopic analysis of CTXB-positive clusters. CTXB relatively specifically binds to MR-enriched ganglioside GM1. The present study demonstrated that TRAIL dose-dependently increased MR clustering in primary cultured CAECs. Our findings are consistent with our previous studies demonstrating that MRs in EC membrane are evenly distributed and CTXB staining displays a random punctuate staining pattern, whereas when ECs were stimulated with death factors including FasL, TNF- α , or endostatin results in the formation of multiple “nonpolarized” CTXB-positive patches [11]. Several previous studies also demonstrated that TRAIL can induce MR clustering in other cell types such as splenocytes and glioblastomas [18, 24, 25]. Together, these findings support the view that MR clustering may serve as a common mechanism for death receptor activation coupled transmembrane signaling. Despite the presence of both TRAIL receptors DR4 and DR5 in MR microdomains in non-endothelial cells [24, 26, 27], the present study only found DR4, but not DR5, in MR clusters after TRAIL stimulation implicating that DR4 is activated by TRAIL and involved in consequent MR clustering in CAECs.

Next, we explored the mechanism by which TRAIL stimulates MR clustering. Ceramide spontaneously fuses MR microdomains to larger ceramide-enriched membrane domains. In this regard, ceramide has been proposed as the driving force in promoting MRs clustering and subsequent signaling pathway in a variety of mammalian cells [9, 10, 28]. Our previous study have demonstrated that ASM activation serves as a triggering mechanism and driving force, leading to fusion of membrane proximal lysosomes into MR clusters on the cell membrane of CAECs in response to FasL, TNF- α and endostatin [11, 16, 22]. In addition, TRAIL-induced MR clustering requires ASM-ceramide signaling in non-endothelial cells such as splenocytes and Jurkat leukemia cells [18, 29]. Consistently, the present study found that TRAIL significantly increased the enrichment of ASM and ceramide in the MR clusters, which was almost completely blocked in *Smpd1*^{-/-} CAECs. These results confirm that ASM aggregation and activation in MR clusters are essential to MR clustering process in CAECs in response to TRAIL. Moreover, our findings further reinforce the concept that ASM activation is a common mechanism mediating MR clustering and corresponding signaling platforms formation in ECs, in particular, upon death receptor activation.

Increasing evidence suggest that MR clustering is able to promote aggregation of NADPH oxidase subunits and to form MR redox signaling platforms after death receptor activation [11, 30–32]. By using confocal microscopy, the present study again demonstrated the formation of such MR redox signaling platforms, which were characterized by aggregation of gp91^{phox} in MR clusters in *Smpd1*^{+/+} CAECs in response to TRAIL activation. Interestingly, in *Smpd1*^{-/-} CAECs, the TRAIL-induced aggregation of NADPH oxidase subunits was abolished. Correspondingly, ESR analysis of $O_2^{\cdot-}$ production also showed that TRAIL-enhanced NADPH oxidase activation in MR clusters was prevented in CAECs with *Smpd1* gene deletion. These results support the view that in CAECs upon TRAIL stimulation, MR clustering is associated with lysosomal ASM-mediated ceramide production and serves as driving force to assemble and activate NADPH oxidase on the EC

membrane. To our knowledge, the present study for the first time reveals that TRAIL triggers lysosomal ASM-mediated MR redox signaling in ECs.

Endothelial dysfunction in small resistance arteries is typically characterized by reduced or loss of endothelium-dependent vasodilation. To this end, the present study demonstrated that TRAIL impairs the endothelium-dependent vasodilator responses in isolated and pressurized small resistance arteries. Our results provide direct evidence that TRAIL produces an early action to induce endothelial dysfunction before detectable apoptotic effect. TRAIL has been reported to induce a detectable apoptosis only with long-term treatment of ECs (>15 hours) [33, 34]. Given a relative resistance of ECs to apoptosis, the functional impairment may represent one of the most important pathological actions of this apoptotic peptide in ECs. Additionally, TRAIL-induced impairment on vasodilator responses was not observed in ASM-deficient arteries indicating that this inhibitory action of TRAIL is associated with lysosomal ASM-mediated formation of MR clusters. Taken together, the results from CAECs and vessel preparation support the view that TRAIL-induced endothelial dysfunction is associated with increased $O_2^{\cdot -}$ production from lysosomal ASM-mediated formation of MR redox signaling platforms. We also found that acetylcholine-induced vasodilation was attenuated by inhibiting nitric oxide (NO) synthase suggesting a NO-dependent vasodilation induced by acetylcholine (data not shown). Thus, increased endothelial $O_2^{\cdot -}$ production by TRAIL could reduce the bioavailability of NO, resulting in impairment of endothelium-dependent vasodilation, as shown in our previous studies and by others [11, 23, 35].

Lysosome trafficking to and fusion with plasma membrane has been identified as an early signaling event in ECs upon death receptor activation [10, 22]. However, there is no direct evidence showing that ASM is actively involved in this fusion process. To this end, we performed more experiments to directly confirm and compare the fusion of lysosomes to plasma membrane in *Smpd1*^{+/+} and *Smpd1*^{-/-} CAECs upon TRAIL stimulation. We found that TRAIL caused colocalization of lysosome marker Lamp-1 with MR clusters on the cell membrane and increased FRET efficiency between MRs and Lamp-1 in *Smpd1*^{+/+} CAECs. Because FRET can only occur between molecules in a distance within a 10-nm range, increased FRET between Lamp-1 and MR component ganglioside G_{M1} should indicate that some lysosomes are indeed fused into cell membrane within MR clusters. We also provided direct evidence that TRAIL triggers lysosome fusion in living cells by using FM1-43, a lysosome specific fluorescence, which can be reversibly quenched by bromide phenol blue (BPB). In quenching experiments, TRAIL was found to cause a decrease in the FM1-43 fluorescence in *Smpd1*^{+/+} CAECs, which was attributable to TRAIL-stimulated lysosome fusion with the plasma membrane, allowing BPB to enter the lysosomes to quench FM1-43 fluorescence. The TRAIL-induced increase in FRET signals and decrease in FM1-43 fluorescence were not observed in *Smpd1*^{-/-} CAECs. Thus, all these direct or indirect evidence strongly suggest that the fusion of lysosomes into the cell plasma membrane occurs in these CAECs on TRAIL stimulation and such TRAIL-induced lysosome fusion requires ASM activity. Our findings are consistent with recent studies showing that ASM was required for the efficient phago-lysosomal fusion [36, 37]. However, lysosomal fusion still occurs in ASM-deficient lymphoblasts but endocytosis and plasma membrane repair were impaired in these cells [38]. Moreover, a recent study showing TCR-triggered fusion of lysosome-type lytic granules is not altered in ASM-deficient cytotoxic T lymphocytes compared to wild-type cells, while in contrast, ASM deficiency results in impaired expulsion of vesicular contents [39]. Most recently, it has been demonstrated that oxidative stress triggered by H_2O_2 induces Ca^{2+} -dependent but ASM-independent lysosome fusion with plasma membrane in Jurkat T cells [40]. It is possible that DR4 activation and H_2O_2 trigger different pathways to activate the ASM, for instance cleavage vs. oxidation, and that these different pathways also show a selective requirement of the ASM for the fusion

process. Nonetheless, these studies suggest that lysosome fusion process may involve ASM-dependent or -independent mechanisms which depend on the cell types and the specific treatment used.

The present study did not attempt to further explore the precise mechanism how ASM contributes to the lysosome fusion process in CAECs. It is possible that TRAIL induces a small amount of ceramide production (kindling ceramide) via activation of ASM in the plasma membrane. This kindling ceramide may trigger lysosome trafficking and fusion to MR microdomains, which result in translocation of more lysosomal ASM onto MRs producing bonfire ceramide. Such bonfire ceramide may function as driving force to promote MR clustering and formation of important signaling platforms, which may further enhance lysosome trafficking and fusion process [10, 41]. Nonetheless, this kindling and bonfire ceramide hypothesis in lysosome-MR associated signaling needs to be tested in the future studies.

In summary, the present study was first to demonstrate that TRAIL is able to induce endothelial dysfunction as an early-stage acute action, which is associated with assembling and activation of NADPH oxidase in MR clusters. The clustered MRs together with activated NADPH oxidase constitutes a redox signaling platform mediating the pathological actions of TRAIL on the vascular endothelium. Finally, we explored an essential role of ASM in the initiation of lysosome trafficking to and fusion with plasma membrane in CAECs. The findings from the present study might increase our understanding how MR redox signaling platforms are formed in ECs. Since death receptor ligands including TRAIL are implicated in the pathogenesis of various cardiovascular diseases such as atherosclerosis, the formation of the redox signaling platforms on the membrane of ECs may mediate the early response of the death receptors leading to endothelial dysfunction *in vivo* and to the development of these diseases.

Acknowledgments

This study was supported by grants from the National Institutes of Health (HL-57244, HL-075316, and HL-091464).

References

1. Schneider P, Bodmer JL, Thome M, Hofmann K, Holler N, Tschopp J. Characterization of two receptors for TRAIL. *FEBS Lett.* 1997; 416:329–334. [PubMed: 9373179]
2. Sheridan JP, Marsters SA, Pitti RM, Gurney A, Skubatch M, Baldwin D, Ramakrishnan L, Gray CL, Baker K, Wood WI, Goddard AD, Godowski P, Ashkenazi A. Control of TRAIL-induced apoptosis by a family of signaling and decoy receptors. *Science.* 1997; 277:818–821. [PubMed: 9242611]
3. Emery JG, McDonnell P, Burke MB, Deen KC, Lyn S, Silverman C, Dul E, Appelbaum ER, Eichman C, DiPrinzio R, Dodds RA, James IE, Rosenberg M, Lee JC, Young PR. Osteoprotegerin is a receptor for the cytotoxic ligand TRAIL. *J Biol Chem.* 1998; 273:14363–14367. [PubMed: 9603945]
4. Secchiero P, Gonelli A, Carnevale E, Milani D, Pandolfi A, Zella D, Zauli G. TRAIL promotes the survival and proliferation of primary human vascular endothelial cells by activating the Akt and ERK pathways. *Circulation.* 2003; 107:2250–2256. [PubMed: 12668516]
5. Secchiero P, Corallini F, di Iasio MG, Gonelli A, Barbarotto E, Zauli G. TRAIL counteracts the proadhesive activity of inflammatory cytokines in endothelial cells by down-modulating CCL8 and CXCL10 chemokine expression and release. *Blood.* 2005; 105:3413–3419. [PubMed: 15644410]
6. Fossati S, Ghiso J, Rostagno A. TRAIL death receptors DR4 and DR5 mediate cerebral microvascular endothelial cell apoptosis induced by oligomeric Alzheimer's Aβ. *Cell Death Dis.* 2012; 3:e321. [PubMed: 22695614]

7. Li JH, Kirkiles-Smith NC, McNiff JM, Pober JS. TRAIL induces apoptosis and inflammatory gene expression in human endothelial cells. *J Immunol.* 2003; 171:1526–1533. [PubMed: 12874246]
8. Alladina SJ, Song JH, Davidge ST, Hao C, Easton AS. TRAIL-induced apoptosis in human vascular endothelium is regulated by phosphatidylinositol 3-kinase/Akt through the short form of cellular FLIP and Bcl-2. *J Vasc Res.* 2005; 42:337–347. [PubMed: 15985761]
9. Zhang Y, Li X, Becker KA, Gulbins E. Ceramide-enriched membrane domains--structure and function. *Biochim Biophys Acta.* 2009; 1788:178–183. [PubMed: 18786504]
10. Grassme H, Jekle A, Riehle A, Schwarz H, Berger J, Sandhoff K, Kolesnick R, Gulbins E. CD95 signaling via ceramide-rich membrane rafts. *J Biol Chem.* 2001; 276:20589–20596. [PubMed: 11279185]
11. Zhang AY, Yi F, Zhang G, Gulbins E, Li PL. Lipid raft clustering and redox signaling platform formation in coronary arterial endothelial cells. *Hypertension.* 2006; 47:74–80. [PubMed: 16344372]
12. Dupree JL, Pomicter AD. Myelin, DIGs, and membrane rafts in the central nervous system. *Prostaglandins Other Lipid Mediat.* 2010; 91:118–129. [PubMed: 19379822]
13. Natoli G, Costanzo A, Guido F, Moretti F, Levrero M. Apoptotic, non-apoptotic, and anti-apoptotic pathways of tumor necrosis factor signalling. *Biochem Pharmacol.* 1998; 56:915–920. [PubMed: 9776301]
14. Zhang AY, Yi F, Jin S, Xia M, Chen QZ, Gulbins E, Li PL. Acid sphingomyelinase and its redox amplification in formation of lipid raft redox signaling platforms in endothelial cells. *Antioxid Redox Signal.* 2007; 9:817–828. [PubMed: 17508908]
15. Jin S, Zhang Y, Yi F, Li PL. Critical role of lipid raft redox signaling platforms in endostatin-induced coronary endothelial dysfunction. *Arterioscler Thromb Vasc Biol.* 2008; 28:485–490. [PubMed: 18162606]
16. Bao JX, Xia M, Poklis JL, Han WQ, Brimson C, Li PL. Triggering role of acid sphingomyelinase in endothelial lysosome-membrane fusion and dysfunction in coronary arteries. *Am J Physiol Heart Circ Physiol.* 2010; 298:H992–H1002. [PubMed: 20061541]
17. Bao JX, Jin S, Zhang F, Wang ZC, Li N, Li PL. Activation of membrane NADPH oxidase associated with lysosome-targeted acid sphingomyelinase in coronary endothelial cells. *Antioxid Redox Signal.* 2010; 12:703–712. [PubMed: 19761405]
18. Dumitru CA, Gulbins E. TRAIL activates acid sphingomyelinase via a redox mechanism and releases ceramide to trigger apoptosis. *Oncogene.* 2006; 25:5612–5625. [PubMed: 16636669]
19. Teng B, Ansari HR, Oldenburg PJ, Schnermann J, Mustafa SJ. Isolation and characterization of coronary endothelial and smooth muscle cells from A1 adenosine receptor-knockout mice. *Am J Physiol Heart Circ Physiol.* 2006; 290:H1713–1720. [PubMed: 16299260]
20. Li JM, Mullen AM, Shah AM. Phenotypic properties and characteristics of superoxide production by mouse coronary microvascular endothelial cells. *J Mol Cell Cardiol.* 2001; 33:1119–1131. [PubMed: 11444917]
21. Boini KM, Xia M, Li C, Zhang C, Payne LP, Abais JM, Poklis JL, Hylemon PB, Li PL. Acid sphingomyelinase gene deficiency ameliorates the hyperhomocysteinemia-induced glomerular injury in mice. *Am J Pathol.* 2011; 179:2210–2219. [PubMed: 21893018]
22. Jin S, Yi F, Zhang F, Poklis JL, Li PL. Lysosomal targeting and trafficking of acid sphingomyelinase to lipid raft platforms in coronary endothelial cells. *Arterioscler Thromb Vasc Biol.* 2008; 28:2056–2062. [PubMed: 18772496]
23. Zhang DX, Yi FX, Zou AP, Li PL. Role of ceramide in TNF-alpha-induced impairment of endothelium-dependent vasorelaxation in coronary arteries. *Am J Physiol Heart Circ Physiol.* 2002; 283:H1785–1794. [PubMed: 12384455]
24. Bellail AC, Tse MC, Song JH, Phuphanich S, Olson JJ, Sun SY, Hao C. DR5-mediated DISC controls caspase-8 cleavage and initiation of apoptosis in human glioblastomas. *J Cell Mol Med.* 2010; 14:1303–1317. [PubMed: 19432816]
25. Song JH, Tse MC, Bellail A, Phuphanich S, Khuri F, Kneteman NM, Hao C. Lipid rafts and nonrafts mediate tumor necrosis factor related apoptosis-inducing ligand induced apoptotic and nonapoptotic signals in non small cell lung carcinoma cells. *Cancer Res.* 2007; 67:6946–6955. [PubMed: 17638906]

26. Xu L, Qu X, Zhang Y, Hu X, Yang X, Hou K, Teng Y, Zhang J, Sada K, Liu Y. Oxaliplatin enhances TRAIL-induced apoptosis in gastric cancer cells by CBL-regulated death receptor redistribution in lipid rafts. *FEBS Lett.* 2009; 583:943–948. [PubMed: 19223002]
27. Rossin A, Derouet M, Abdel-Sater F, Hueber AO. Palmitoylation of the TRAIL receptor DR4 confers an efficient TRAIL-induced cell death signalling. *Biochem J.* 2009; 419:185–192. [PubMed: 19090789]
28. Goni FM, Alonso A. Membrane fusion induced by phospholipase C and sphingomyelinases. *Biosci Rep.* 2000; 20:443–463. [PubMed: 11426688]
29. Min Y, Shi J, Zhang Y, Liu S, Liu Y, Zheng D. Death receptor 5-recruited raft components contributes to the sensitivity of Jurkat leukemia cell lines to TRAIL-induced cell death. *IUBMB Life.* 2009; 61:261–267. [PubMed: 19242990]
30. Yang B, Rizzo V. TNF-alpha potentiates protein-tyrosine nitration through activation of NADPH oxidase and eNOS localized in membrane rafts and caveolae of bovine aortic endothelial cells. *Am J Physiol Heart Circ Physiol.* 2007; 292:H954–962. [PubMed: 17028163]
31. Shao D, Segal AW, Dekker LV. Lipid rafts determine efficiency of NADPH oxidase activation in neutrophils. *FEBS Lett.* 2003; 550:101–106. [PubMed: 12935894]
32. Samhan-Arias AK, Garcia-Bereguian MA, Martin-Romero FJ, Gutierrez-Merino C. Clustering of plasma membrane-bound cytochrome b5 reductase within 'lipid raft' microdomains of the neuronal plasma membrane. *Mol Cell Neurosci.* 2009; 40:14–26. D. [PubMed: 18973815]
33. Zauli G, Pandolfi A, Gonelli A, Di Pietro R, Guarnieri S, Ciabattini G, Rana R, Vitale M, Secchiero P. Tumor necrosis factor-related apoptosis-inducing ligand (TRAIL) sequentially upregulates nitric oxide and prostanoid production in primary human endothelial cells. *Circ Res.* 2003; 92:732–740. [PubMed: 12649264]
34. Di Pietro R, Mariggio MA, Guarnieri S, Sancilio S, Giardinelli A, Di Silvestre S, Consoli A, Zauli G, Pandolfi A. Tumor necrosis factor-related apoptosis-inducing ligand (TRAIL) regulates endothelial nitric oxide synthase (eNOS) activity and its localization within the human vein endothelial cells (HUVEC) in culture. *J Cell Biochem.* 2006; 97:782–794. [PubMed: 16229016]
35. Heylen E, Huang A, Sun D, Kaley G. Nitric oxide-mediated dilation of arterioles to intraluminal administration of aldosterone. *J Cardiovasc Pharmacol.* 2009; 54:535–542. [PubMed: 19770672]
36. Schramm M, Herz J, Haas A, Kronke M, Utermohlen O. Acid sphingomyelinase is required for efficient phago-lysosomal fusion. *Cell Microbiol.* 2008; 10:1839–1853. [PubMed: 18485117]
37. Utermohlen O, Herz J, Schramm M, Kronke M. Fusogenicity of membranes: the impact of acid sphingomyelinase on innate immune responses. *Immunobiology.* 2008; 213:307–314. [PubMed: 18406376]
38. Tam C, Idone V, Devlin C, Fernandes MC, Flannery A, He X, Schuchman E, Tabas I, Andrews NW. Exocytosis of acid sphingomyelinase by wounded cells promotes endocytosis and plasma membrane repair. *J Cell Biol.* 2010; 189:1027–1038. [PubMed: 20530211]
39. Herz J, Pardo J, Kashkar H, Schramm M, Kuzmenkina E, Bos E, Wiegmann K, Wallich R, Peters PJ, Herzig S, Schmelzer E, Kronke M, Simon MM, Utermohlen O. Acid sphingomyelinase is a key regulator of cytotoxic granule secretion by primary T lymphocytes. *Nat Immunol.* 2009; 10:761–768. [PubMed: 19525969]
40. Li X, Gulbins E, Zhang Y. Oxidative Stress Triggers Ca-Dependent Lysosome Trafficking and Activation of Acid Sphingomyelinase. *Cell Physiol Biochem.* 2012; 30:815–826. [PubMed: 22890197]
41. Yu C, Alterman M, Dobrowsky RT. Ceramide displaces cholesterol from lipid rafts and decreases the association of the cholesterol binding protein caveolin-1. *J Lipid Res.* 2005; 46:1678–1691. [PubMed: 15863835]

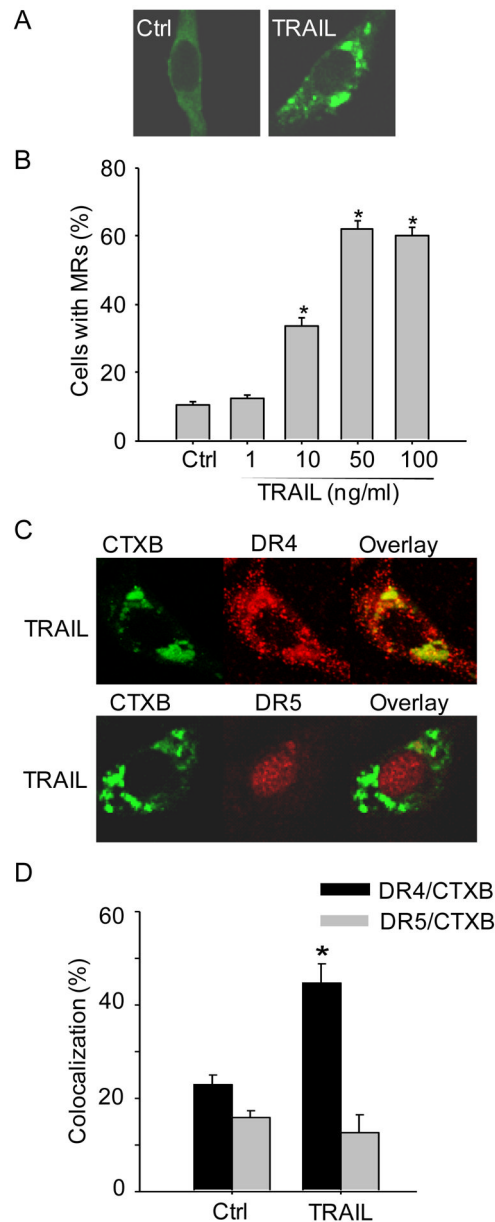


Figure 1. TRAIL induces MR clustering in mouse CAECs via DR4 receptor

(A) Representative confocal images showing TRAIL induced clustering of MR markers ganglioside GM1, which were detected by cholera toxin subunit B (CTXB). (B) Summarized data showing the dose-dependent effect of TRAIL (0–100 ng/ml) on MR clustering in *Smpd1*^{+/+} CAECs (n=6). (C) Confocal microscopy of *Smpd1*^{+/+} CAECs revealed a co-localization of DR4 but not DR5 with MR clusters upon TRAIL stimulation. (D) Summarized data showing the co-localization between MRs and DR4 or DR5 in mouse *Smpd1*^{+/+} CAECs. **P* < 0.05 vs. control (n=6).

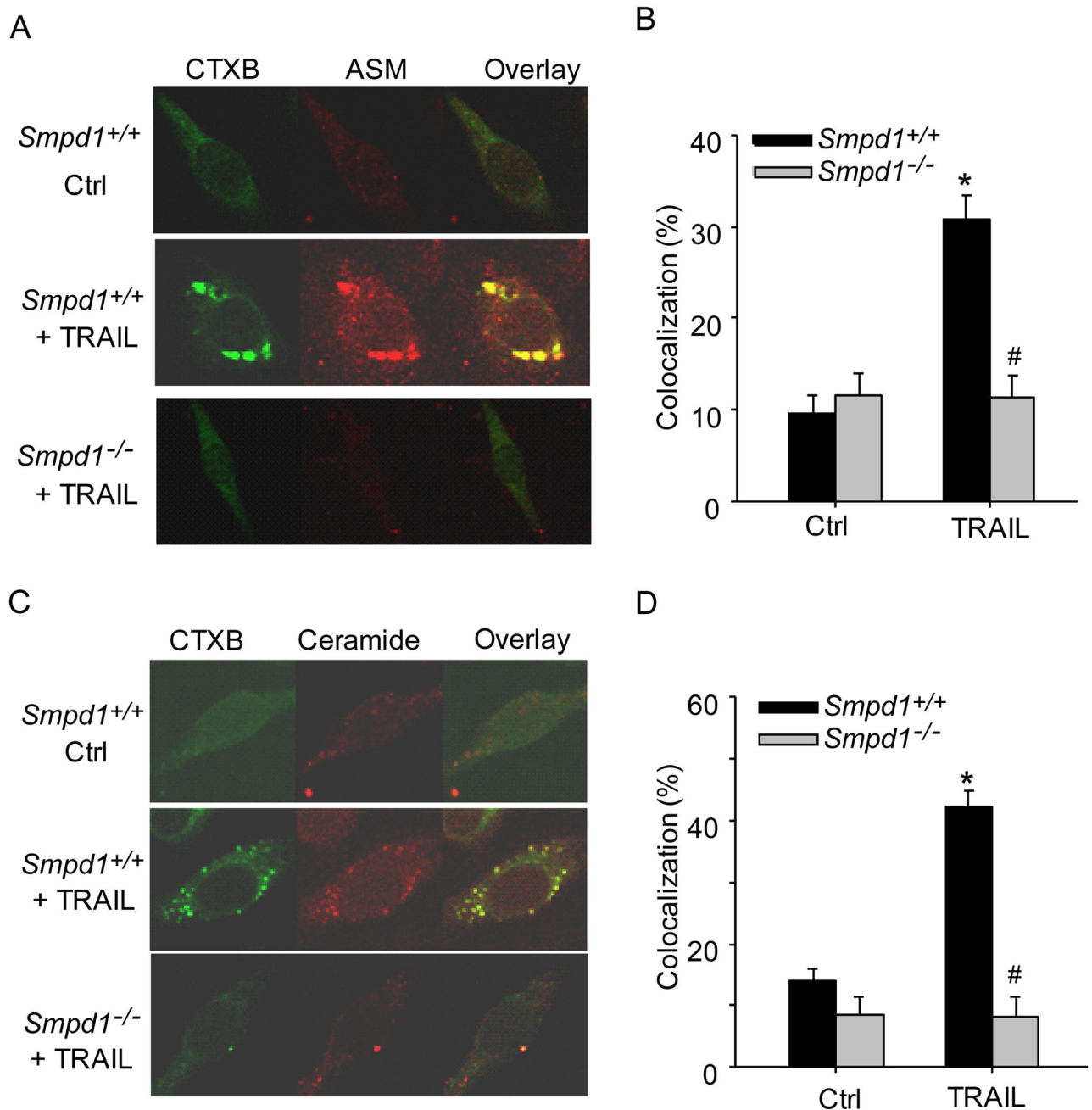


Figure 2. TRAIL triggers translocation of ASM to MR domains in mouse CAECs
 (A) Representative confocal images depicting the effect of TRAIL on the co-localization between MRs (detected by CTXB) and ASM in *Smpd1*^{+/+} and *Smpd1*^{-/-} CAECs. (B) Displaying are the summarized data showing the colocalization between MRs and ASM. (C) Representative confocal images depicting the effect of TRAIL on the co-localization between MRs and ceramide in *Smpd1*^{+/+} and *Smpd1*^{-/-} CAECs. (D) Displaying are the summarized data showing the colocalization between MRs and ceramide from six independent experiments. * $P < 0.05$ vs. *Smpd1*^{+/+} control; # $P < 0.05$ vs. *Smpd1*^{+/+} TRAIL (n=6).

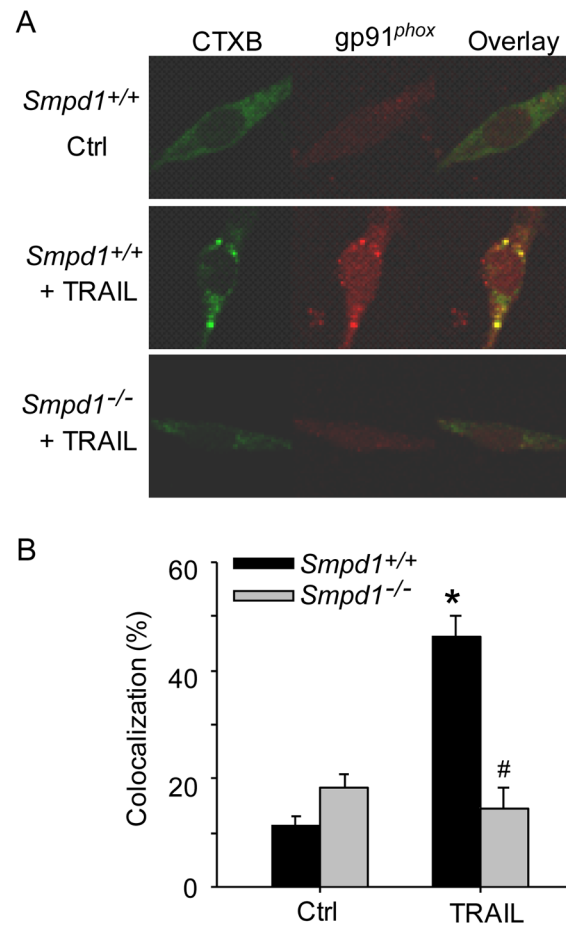


Figure 3. ASM deficiency abolishes TRAIL-induced clustering of NADPH oxidase subunits gp91^{phox} in MR domains in CAECs

(A) Representative confocal fluorescence images showing the colocalization between MRs and gp91^{phox} in *Smpd1*^{+/+} and *Smpd1*^{-/-} CAECs. (B) Displaying are the summarized data showing the colocalization between MRs and gp91^{phox} from six independent experiments. **P* < 0.05 vs. *Smpd1*^{+/+} control; #*P* < 0.05 vs. *Smpd1*^{+/+} TRAIL (n=6).

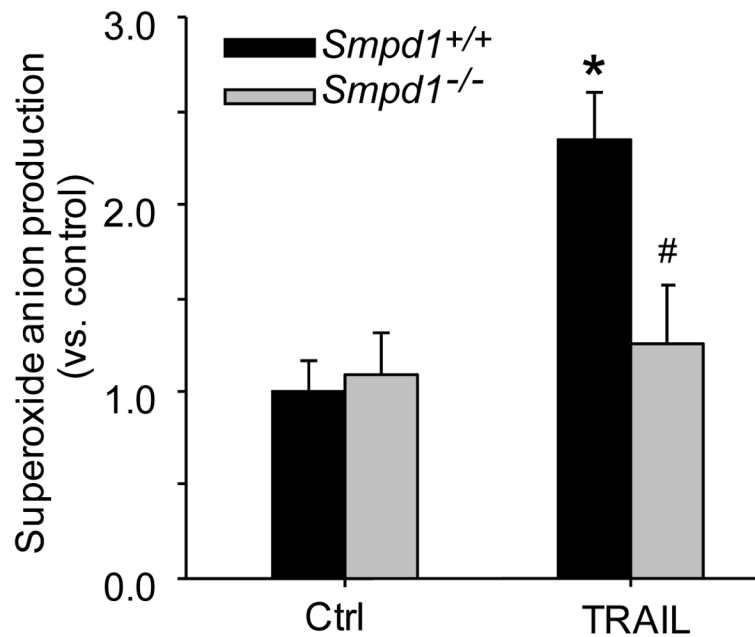


Figure 4. Reduction of TRAIL-induced $O_2^{\cdot -}$ production in ASM-deficient CAECs
 CAECs were stimulated with or without TRAIL and then incubated with $O_2^{\cdot -}$ -specific spin trap 1-hydroxy-3-methoxycarbonyl-2,2,5,5-tetramethylpyrrolidine (CMH) to form more stable free radicals (CMH- $O_2^{\cdot -}$), which was immediately analyzed by electron spin resonance spectrometry (ESR). Summarized data showing the effect of TRAIL on $O_2^{\cdot -}$ production in *Smpd1*^{+/+} and *Smpd1*^{-/-} CAECs., * $P < 0.05$ vs. *Smpd1*^{+/+} control; # $P < 0.05$ vs. *Smpd1*^{+/+} TRAIL (n=6).

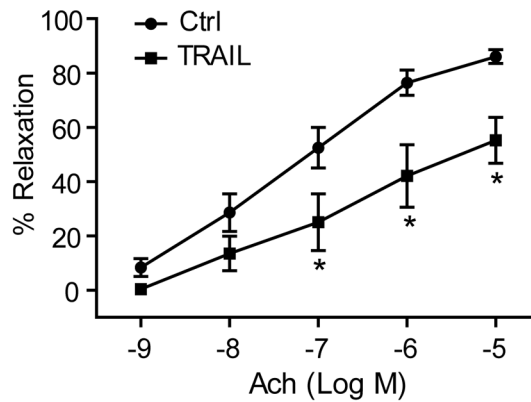
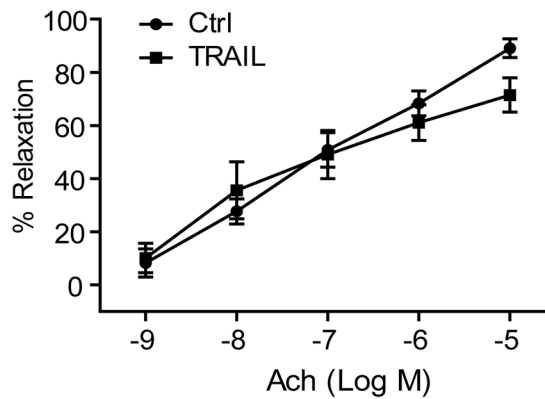
A *Smpd1*^{+/+} arteriesB *Smpd1*^{-/-} arteries

Figure 5. Effect of TRAIL on concentration-dependent vasodilator response in freshly isolated and pressurized mouse arteries

(A) Summarized data showing that pretreatment with TRAIL significantly attenuated acetylcholine (Ach)-induced endothelium-dependent relaxation in small arteries isolated from *Smpd1*^{+/+} mice. (B) Summarized data showing that pretreatment with TRAIL had no inhibitory effect on acetylcholine (Ach)-induced endothelium-dependent relaxation in small arteries isolated from *Smpd1*^{-/-} mice. **P*<0.05 vs. *Smpd1*^{+/+} control (n=6 mice).

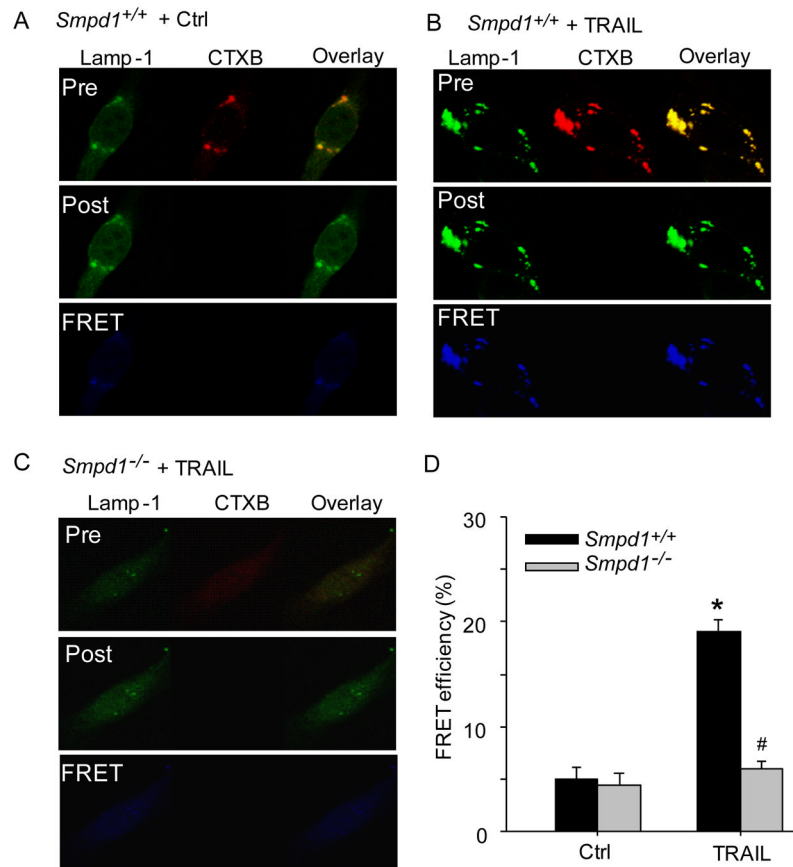


Figure 6. TRAIL increases expression of lysosome marker Lamp-1 in MR clusters in CAECs (A–C) Representative confocal images of fluorescence resonance energy transfer (FRET) between FITC-Lamp-1 and TRITC-CTXB in *Smpd1*^{+/+} CAECs treated with vehicle control (PBS buffer only) (A), TRAIL (B), or in *Smpd1*^{-/-} CAECs with TRAIL. The FRET images were obtained by subtraction of the pre-bleaching images from the post-bleaching images and shown in dark blue color. Increased intensity of blue color represents higher level of FRET in these cells. (D) Displaying are the summarized data showing the effect of TRAIL on FRET efficiency between FITC-Lamp-1 and TRITC-CTXB in *Smpd1*^{+/+} and *Smpd1*^{-/-} CAECs. * $P < 0.05$ vs. *Smpd1*^{+/+} control; # $P < 0.05$ vs. *Smpd1*^{+/+} TRAIL (n=6).

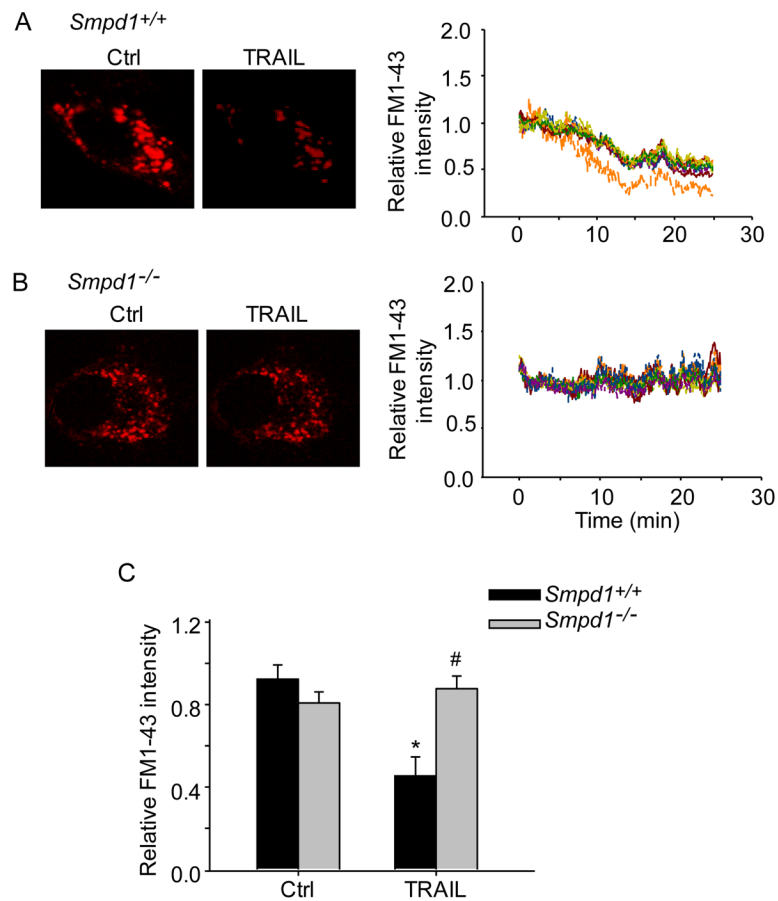


Figure 7. Blockade of TRAIL-induced lysosome fusion with plasma membrane in ASM-deficient CAECs

CAECs were first loaded with FM1-43, a lysosome specific fluorescence probe, and then incubated in fresh medium containing bromide phenol blue (BPB), which reversibly quenches FM1-43 fluorescence. In quenching experiments, lysosome fusion with the plasma membrane will allow BPB to enter the lysosomes to quench FM1-43 fluorescence. (A) Left panel: representative confocal fluorescence images of FM1-43 fluorescence in *Smpd1*^{+/+} CAECs before and after treatment with TRAIL. Right panel: representative traces of TRAIL-induced changes of FM1-43 fluorescence, normalized to that obtained before TRAIL treatment. (B) Left panel: representative confocal fluorescence images of FM1-43 fluorescence quenching in *Smpd1*^{-/-} CAECs treated with TRAIL. Right panel: representative traces of TRAIL-induced changes of FM1-43 fluorescence in *Smpd1*^{-/-} CAECs. (C) Summarized data showing the effect of TRAIL on FM1-43 fluorescence quenching in *Smpd1*^{+/+} and *Smpd1*^{-/-} CAECs. **P*<0.05 vs. *Smpd1*^{+/+} control (n=6); #*P*<0.05 vs. *Smpd1*^{+/+} TRAIL (n=6).